Noncentrosymmetric Cu(II) Layered Hydroxide: Synthesis, Crystal Structure, Nonlinear Optical, and Magnetic Properties of Cu 2 (OH) 3 (C 12 H 25 SO 4)

Quentin Evrard, Cédric Leuvrey, Pierre Farger, Émilie Delahaye, Pierre Rabu, Gregory Taupier, Kokou Dodzi Dorkenoo, Jean-Michel Rueff, Nicolas Barrier, Olivier Pérez, et al.

A non-centrosymmetric Cu(II) layered hydroxide: synthesis, crystal structure, non-linear optical and magnetic properties of $Cu_2(OH)_3(C_{12}H_{25}SO_4)$

*Quentin Evrard,[a] Cédric Leuvrey,[a] Pierre Farger,[a] Emilie Delahaye,[a] Pierre Rabu,[a] Grégory Taupier,[a] Kokou Dodzi Dorkenoo,[a] Jean-Michel Rueff,[b] Nicolas Barrier,[b] Olivier Pérez,[b] Guillaume Rogez[a] **

[a] Institut de Physique et Chimie de Strasbourg, Université de Strasbourg and CNRS, UMR 7504, 23 rue du Loess, BP43, 67034 Strasbourg cedex, France

[b] Laboratoire de Cristallographie et Sciences des Matériaux, UMR CNRS 6508, 6 Boulevard du Maréchal Juin, 14050 Caen cedex 4, France

Keywords. Layered Simple Hydroxide, dodecylsulfate, copper, morphology, non-centrosymmetric, non-linear optics

Abstract. Single-crystals of the layered copper hydroxide dodecylsulfate $Cu_2(OH)_3(C_{12}H_{25}SO_4)$ have been obtained for the first time, by controlled hydrolysis of an aqueous copper acetate solution. Interestingly this compound crystallizes in a non-centrosymmetric space group ($P2_1$, a = 5.591(10) Å, b = 6.108(11) Å, c = 26.96(5) Å, $\alpha = \gamma = 90°$, $\beta = 92.76°$), which is further confirmed by non-linear optical measurements. Within the course of the synthesis, a probable intermediate

between $Cu(OAc)_2 \cdot H_2O$ and the layered $Cu_2(OH)_3(C_{12}H_{25}SO_4)$ was isolated and characterized. X-ray structure analysis showed that this intermediate presents a ribbon-like structure, of formula $Cu_3(C_{12}H_{25}SO_4)_2(CH_3COO)_2(OH)_2(H_2O)_2$. The magnetic properties of the layered $Cu_2(OH)_3(C_{12}H_{25}SO_4)$ have been analyzed in the high-temperature region ($T > 20$ K) by considering a high-temperature series expansion for a S = ½ Heisenberg 2D triangular lattice. At lower temperature, the compound shows a 3D antiferromagnetic ordering (T_N = 10.8 K). The ribbon-like compound $Cu_3(C_{12}H_{25}SO_4)_2(CH_3COO)_2(OH)_2(H_2O)_2$ presents an overall antiferromagnetic behaviour, resulting from a combination of ferro and antiferromagnetic interactions between nearest neighbours within the chains.

Introduction.

Layered materials have long proved to be materials of choice in the field of organic-inorganic hybrid systems.[1,2] Among these materials, one may quote layered oxalate,[3] Layered Double or Simple Hydroxides (LDH[4] or LSH[5]), clays,[6,7] hexathiohypodiphosphates (MPS_3),[8,9] layered perovskite[10] or MX_4-based layered perovskite-like materials.[11] Hybrid materials based on these systems can have interesting properties in magnetism,[3,5,12,13] ferroelectricity,[14] multiferroicity,[15–17] magnetoelectricity,[18] luminescence,[19,20] trapping of molecular species,[21,22] anti-corrosion[23] or catalysis[24] for instance.

In this respect, Layered Hydroxides are particularly interesting because they can be functionalized by various anionic molecules. LDH and LSH possess a similar hydrotalcite structure but they essentially differ in their composition and in the charge of the inorganic layers. LDHs are synthetic anionic clays, of formula $[M^{II}_{(1-x)},M^{III}_x(OH)_2][A^{n-}_{(x/n)}(H_2O)]$ (M^{II} = Mg, Co, Ni, Zn,…; M^{III} = Al, Cr, V, Ga, Rh,…). The positive charge of the hydrotalcite $[M(OH)_2]$ layers

is compensated by anionic species located in the interlayer space. They can be functionalized by exchange of these A^{n-} anions.[4] LSH contains only divalent transition metal ions, with a formula $M_2(OH)_{4-nx}(A^{n-})_x$ (M^{II} = Co, Cu, Ni, Mn, … and A^{n-} = carboxylate, sulfate, sulfonate or phosphonate anion). Inserted anion A is coordinated to the inorganic layers, which are thus neutral.

Several strategies have been reported for the synthesis of functionalized LSH: insertion-grafting,[25–28] direct hydrothermal synthesis,[29,30] *in situ* synthesis,[31] controlled hydrolysis[32] or, very recently, confined condensation.[33] The most widely used method is insertion-grafting, which consists in an anionic exchange between the starting layered hydroxy-acetate and the molecule of interest bearing an anchoring group (carboxylate, sulfonate or phosphonate).[5,18] A pre-intercalation method has been shown to be very effective to allow the insertion-grafting of large, hydrophobic or prone to hydrolysis molecules, including coordination complexes in Layered Simple Hydroxides.[25,26,34,35] This method consists in the insertion-grafting of molecules bearing long-alkyl chains by anion-exchange from the starting layered hydroxy-acetate. In the case of layered copper hydroxide, dodecyl sulfate can be readily inserted into copper hydroxy-acetate, much more easily than less flexible molecules. Compared to copper hydroxy-acetate, copper hydroxy-dodecylsulfate presents a much larger and more hydrophobic interlamellar spacing which enables the subsequent insertion of various molecules.

The precise understanding of the properties of the layered hybrid compounds (optical, magnetic or dielectric for instance) requires a deeper knowledge of their structure. To this aim, it is worth investigating the structures of the starting materials, which appears not to be an easy task. The single-crystal structure of copper hydroxy-acetate $Cu_2(OH)_3(OAc)\cdot H_2O$ was only reported in 2011, whereas research involving this compound has been performed for more than 25 years.[5,27,28,36–41] Concerning the dodecylsulfate analogue, now widely used as a starting compound

for insertion, to the best of our knowledge, no precise description of its structure has ever been reported.

We describe here the synthesis of high crystallinity $Cu_2(OH)_3(C_{12}H_{25}SO_4)$. Single-crystal structure determination shows that this compound crystallizes in the non-centrosymmetric space group $P2_1$. The non-centrosymmetry is confirmed by non-linear optical measurements. Moreover, during the synthetic approach, we managed to isolate and to characterize by single-crystal X-ray diffraction a ribbon-like compound of formula $Cu_3(C_{12}H_{25}SO_4)_2(CH_3COO)_2(OH)_2(H_2O)_2$ which can be considered as an intermediate in the synthesis of $Cu_2(OH)_3(C_{12}H_{25}SO_4)$ from $Cu(CH_3COO)_2{\cdot}H_2O$. Finally, the magnetic properties of $Cu_3(C_{12}H_{25}SO_4)_2(CH_3COO)_2(OH)_2(H_2O)_2$ and $Cu_2(OH)_3(C_{12}H_{25}SO_4)$ are described. $Cu_3(C_{12}H_{25}SO_4)_2(CH_3COO)_2(OH)_2(H_2O)_2$ presents a combination of ferro and antiferromagnetic interactions between nearest neighbours within the chains, whereas the properties of $Cu_2(OH)_3(C_{12}H_{25}SO_4)$, which presents an antiferromagnetic ordering at T_N = 10.8 K, can be interpreted in the high-temperature regime ($T > 20$ K) using a Heisenberg 2D triangular spin lattice model.

Experimental Section.

Synthesis of $Cu_2(OH)_3(CH_3COO){\cdot}H_2O$, ($Cu_2(OH)_3(OAc){\cdot}H_2O$) : The synthesis is adapted from the one of Švarcová *et al.*[42] 4 g (20 mmol) of $Cu(CH_3COO)_2{\cdot}H_2O$ are solubilized in 100 mL of a mixture water/ethanol (90/10 v:v), then heated under reflux at 60°C during 72 h. Blue-green crystals are then collected by filtration and washed with water and ethanol. The filtrate is then heated again at 60°C for 48 h, and the blue green crystals are collected, washed with water and ethanol and mixed with the first fraction. This procedure is repeated twice. Yield: *ca.* 4%.

Synthesis of $Cu_3(C_{12}H_{25}SO_4)_2(CH_3COO)_2(OH)_2(H_2O)_2$ (1) : $Cu(OAc)_2 \cdot H_2O$ is added to 0.5 equivalent of a solution (0.05 M) of $C_{12}H_{25}SO_4Na$ in a water/ethanol mixture (70/30 v:v), stirred vigorously during 1 h at room temperature and let slowly evaporated at room temperature without stirring. Small crystalline needles grow within a few days (3 days for a total volume of 100 mL). Yield: *ca.* 30%.

Synthesis of $Cu_2(OH)_3(C_{12}H_{25}SO_4)$, ($Cu_2(OH)_3(DS)$) (2) : 1.33 g (5 mmol) of sodium dodecylsulfate are dissolved in 100 mL of a water/ethanol mixture (70/30 v:v). $Cu(OAc)_2 \cdot H_2O$ (2 g, 10 mmol) are added to the solution which is stirred during 1 h. The mixture is then heated under reflux at 60°C for 3 days, without stirring. The blue solid is filtered, washed three times with water, twice with a water/ethanol mixture and once with ethanol, then dried under vacuum. Yield: 40% (based on NaDS) (885 mg, 2 mmol).

The Powder X-Ray Diffraction (PXRD) diagram of $Cu_2(OH)_3(C_{12}H_{25}SO_4) \cdot$(**2**) was measured in transmission geometry on a PANalytical X'Pert PRO diffractometer equipped with a focusing mirror (Cu-$\lambda K\alpha_{moy}$) and a PIXcel detector. The polycrystalline sample was loaded in a capillary of 0.3 mm diameter. The PXRD diagram was recorded at room temperature between 3 and 60°(2θ) with a step size of ~0.013°(2θ) for 2 hours. The Rietveld refinements were performed with the JANA2006 program[43] to check the composition of the polycrystalline sample of $Cu_2(OH)_3(C_{12}H_{25}SO_4)$. Assuming the crystal structure model obtained from the single crystal X-ray data only the scale, unit cell and profile parameters were refined. The low *R* factors (R_{obs} = 7,01 ; R_{Bobs} = 13,15 ; R_{wp} = 8,43, *gof* = 1,80) and the absence of any extra peaks testify that the polycrystalline sample correspond to a single-phase sample of $Cu_2(OH)_3(C_{12}H_{25}SO_4)$ (Figure S1).

Powder X-ray diffraction (XRD) patterns of the ribbon-like compounds (compound **1**, Figure S2) were collected with a Bruker D8 diffractometer (Cu Kα1 = 0.1540598 nm) equipped with a LynxEye detector discriminating in energy.

Single crystal X-ray diffraction measurements were performed using Mo $K\alpha$ radiation produced with a micro focus Incoatec Iμs sealed X-ray tube on a KappaCCD (Bruker-Nonius) four circles diffractometer equipped with an Apex2 bi-dimensional detector (CCD: charge coupled device). Crystals of suitable crystalline quality were selected for single crystal XRD; details of the data collection are given in Table 1. Data were corrected from absorption using Sadabs program developed for scaling and absorption corrections of area detector data.[44,45] The structure was determined with Superflip[46] using charge-flipping algorithm and introduced in the program Jana2006.[43]

FT-IR spectra of the hybrid compounds were collected in ATR mode on a SpectrumII spectrometer (PerkinElmer). TGA-TDA experiments were performed using a TA instrument SDT Q600 (heating rates of 5°C·min^{-1} under air stream, using Pt crucibles). The SEM images were obtained with a JEOL 6700F microscope equipped with a field emission gun, operating at 3 kV in the SEI mode and with a ZEISS GeminiSEM 500 microscope, operating at 1 kV or 5kV in secondary electron imaging mode. The magnetic studies were carried out with a SQUID magnetometer (Quantum Design MPMS3) covering the temperature and field ranges 2–300 K and +/– 7 T, respectively. Magnetization versus field measurements at room temperature confirm the absence of ferromagnetic impurities. Data were corrected for the sample holder, and diamagnetism was estimated from Pascal constants.

Non-Linear Optical (NLO) activity was evaluated by detecting the Second-Harmonic Generation (SHG) process. SHG measurements have been performed with an inverted microscope (Olympus IX71). The SHG process is induced by focusing in the sample a pulsed laser beam at 900 nm (Spectra Physics, Tsunami) with ultrashort pulse durations (100 fs at 80 MHz) and input power of 50 mW. Samples in powder form deposited onto a microscope slide are excited by this laser beam using a low-aperture microscope objective (Olympus, SLMPlan, X20, N.A. = 0.35). The SHG signal emitted at 450 nm is separated from the excitation beam by a dichroic mirror and collected during 1 s in reflection mode using a spectrometer (Acton research SP2300) coupled with a CCD camera (Princeton Instruments PIXIS400). For SHG imaging, a micrometric displacement stage is combined with a photon photomultiplier in counting mode (Hamamatsu, H7421).

Results and discussion

Syntheses and crystal structures

Since it is possible to obtain $Cu_2(OH)_3(OAc)\cdot H_2O$ as single crystals,[42] and considering that anionic exchange reactions from $Cu_2(OH)_3(OAc)\cdot H_2O$ have been well studied,[5] including for the synthesis of $Cu_2(OH)_3(C_{12}H_{25}SO_4)$,[41] we first tried to obtain single crystals of $Cu_2(OH)_3(C_{12}H_{25}SO_4)$ by single-crystal to single-crystal modification from $Cu_2(OH)_3(OAc)\cdot H_2O$. In order to maximize the chance to keep the crystallinity of the starting material, we performed exchange reaction from $Cu_2(OH)_3(OAc)\cdot H_2O$ without stirring and using softer condition than for the classical exchange (25°C during 48 h instead of 60°C during 72 h). Yet we could obtain only partial exchange (Figure S3) and even though the crystallinity remains very good (Figure S4), the single-crystal character is lost.

Therefore, we adopted another method, derived from the one described by Švarcová *et al.* which has enabled to obtain single crystals of $Cu_2(OH)_3(CH_3COO)\cdot H_2O$,[42] or from the one used by Fujita to obtain single crystals of copper hydroxides with sulfonates, either with a layer structure or with a distorted diamond chain structure.[32,47] In the present case, it consists in adding copper acetate to a solution of sodium dodecylsulfate in a water/ethanol mixture heating the solution at 70°C for several days. Despite the relative simplicity of this procedure, several observations can be made.

When the two reactants are mixed (either solid $Cu(OAc)_2\cdot H_2O$ or concentrated aqueous solution of $Cu(OAc)_2\cdot H_2O$ added to 0.5 equivalent of a solution (0.05 M) of $C_{12}H_{25}SO_4Na$ in a water/ethanol (70/30 v:v) mixture, or the reverse, $C_{12}H_{25}SO_4Na$ poured onto solid $Cu(OAc)_2\cdot H_2O$ or into concentrated aqueous solution of $Cu(OAc)_2\cdot H_2O$), a blueish precipitate forms immediately. This precipitate is filtered after 1 h of stirring at room temperature. Powder X-ray diffraction (Figure S2) and infrared spectroscopy (Figure S5) clearly show that this blueish precipitate is composed of sodium dodecylsulfate and at least one other phase which could not be identified and which corresponds neither to copper acetate nor to copper dodecylsulfate nor to the ribbon-like structure which forms when the suspension is let evaporate (see below).

Indeed, when, instead of being filtered, this suspension is slowly evaporated at room temperature without stirring, crystalline needles form (compound **1**) (Figure 1 left). Interestingly, when the reactants are only mixed during 5 min, without full dissolution of $Cu(OAc)_2\cdot H_2O$, similar needles appear to grow from the remaining $Cu(OAc)_2\cdot H_2O$ crystals (compound **1'**) (Figure 1 right), which suggests that the corresponding compound may be an intermediate between $Cu(OAc)_2\cdot H_2O$ and $Cu_2(OH)_3(DS)$.

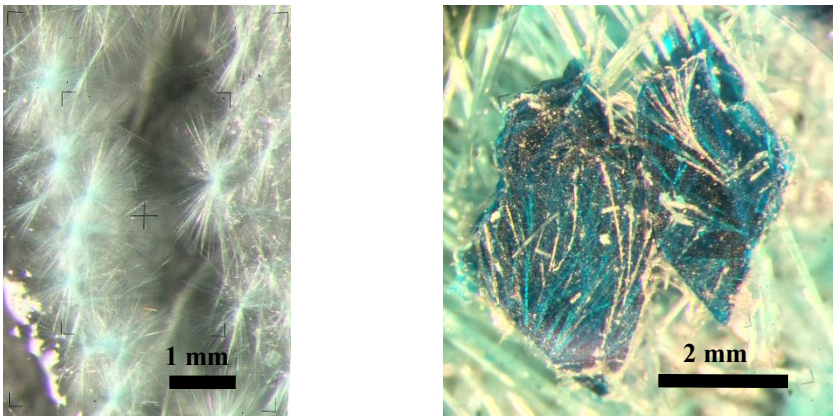

Figure 1. Optical microscopy image of the crystals of compound **1** (left) and of compound **1'** (right).

Single-crystal structure determination on the needles showed that compounds **1** and **1'** are in fact identical. The crystal structure of compound **1** can be described by 2 Cu, 1 S, 8 O, 14 C independent atoms. All the atomic positions were refined and then atomic displacement parameters (ADP) were considered as anisotropic for copper and sulfur atoms and isotropic for all remaining atoms. At this step, 25 independent hydrogen atoms were introduced using geometric considerations to fill the carbon environment. Bond valence sum calculations performed for all the atoms lead to low value for two O atoms: O2 and O3 (0.4 and 1.3 respectively); these weak values can be attributed to the presence of H atoms. Two hydrogen atoms were then added around O2 and one hydrogen around O3; the position of the H atoms was determined based on geometrical considerations and restricted in link to their O first neighbour. The resulting model corresponds to the composition $Cu_3(C_{12}H_{25}SO_4)_2(CH_3COO)_2(OH)_2(H_2O)_2$, where 2 water molecules and 2 hydroxide groups per formula are present. Final reliability factors and details of the refinement are reported in Table 1 and the atomic parameters of compound **1** are summarized in Tables S1a and S1b.

Table 1. Crystallographic data for **1**(**1'**) and **2**.

sample	**1**	**2**
Chemical formula	$Cu_3(C_{12}H_{25}SO_4)_2(CH_3COO)_2(OH)_2(H_2O)_2$	$Cu_2(OH)_3(C_{12}H_{25}SO_4)$
Molecular weight (g.mol^{-1})	905.5	444.5
Space group	$P\bar{1}$	$P2_1$
a (Å)	5.602(2)	5.591(10)
b (Å)	8.314(3)	6.108(11)
*c (*Å)	21.283(8)	26.96(5)
α (°)	83.02(2)	90
β (°)	85.87(2)	92.76(3)
γ (°)	81.85(2)	90
Cell volume (Å^3)	972.4(7)	920(3)
Z	1	2
Density (g.cm^{-3})	*1.546*	*1.6053*
μ (mm^{-1})	*1.798*	*2.452*
wavelength (Å)	0.71069	0.71069
scan strategy / Dx (mm)	*ω/φ scan / 50*	*ω/φ scan / 50*
Θ max	29.17	29.03
Reflections index limit	-6≤ h ≤7 -10≤ k ≤ 11 -27≤ h ≤ 28	-7≤ h ≤7 -8≤ k ≤ 8 -36≤ h ≤ 36
unique reflections with I≥3σ(I)	1199	1093
Absorption correction	multi-scan / SADABS	multi-scan / SADABS
Internal R value before /after correction (%)	15.1% / 6.2%	15.3% / 4.9%
# refinement parameters	119	78
ρmin / *ρmax* (*e*/ Å ^{3})	-1.72/1.21	-2.43/1.19
F(000)	473	460
Reliability factors %	9.95%	6.98%

Compound **1** adopts a distorted diamond chain structure, analogous to that of azurite $Cu_3(OH)_2(CO_3)_2$.[48] A similar arrangement has been described by Fujita *et al.* for sulfonate compounds of general formula $Cu_3(OH)_2(RSO_3)_2(CH_3COO)_2(H_2O)_2$,[47] but, to the best of our knowledge, it is the first time such a structure is reported with sulfate groups. Although the general diamond-like structure of the chains remains essentially the same, it is worth underlining here that in the present case, the sulfate groups are mono-coordinated to one copper atoms, whereas the sulfonate groups in the compounds described by Fujita *et al.* are, depending on the nature of the alkyl chain, either coordinated in μ_2 bridging mode to two copper ions or not coordinated (instead, water molecules are coordinated in μ_2 bridging mode). The chains in **1**, well separated from each other by the dodecyl groups, develop along the *a* direction (Figure 2).

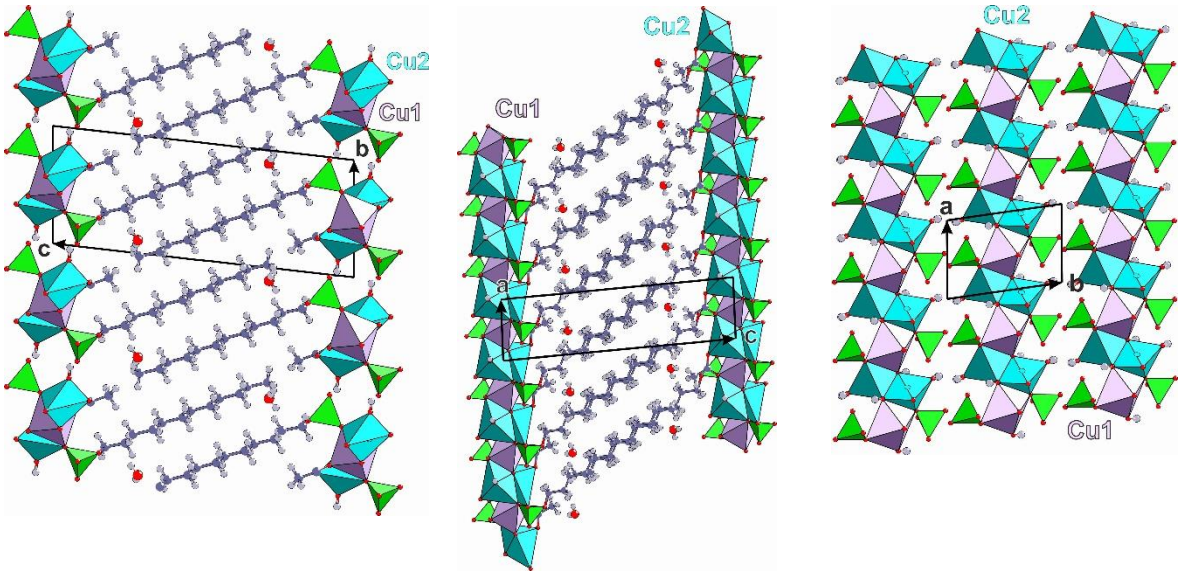

Figure 2. View of the structure of $Cu_3(C_{12}H_{25}SO_4)_2(CH_3COO)_2(OH)_2(H_2O)_2$ (**1**) along the *a* (left) and *b* (middle) axis. Structure of the inorganic layer, (*ab*) plane (right). Cu (purple (Cu1) and blue (Cu2)), O (red), S (green), C (grey), H (white).

Both crystallographically independent copper atoms are octahedrally coordinated by oxygen atoms. Hydroxide groups are in μ_3 bridging coordination mode and bridge one Cu1 and two Cu2.

Acetate groups are in (κ^1-(κ^1-μ_2))-μ_3 bridging mode are coordinated to one Cu1 in κ^1 mode and bridge one Cu1 and one Cu2 in κ^1-μ_2 mode. Finally, the sulfate groups are bridging one Cu1 and one Cu2 in κ^1-μ_2 mode. One water molecule completes the coordination sphere of Cu2.

If, using the same starting conditions, the solution is heated at 60°C without stirring and with a condenser during 3 days instead of being slowly evaporated, blue platelet-like crystals form with a relatively high yield (around 40%). Despite the very thin plate-like shape, the structure could be solved on a single crystal. The compound is a layered copper hydroxide of formula $Cu_2(OH)_3(C_{12}H_{25}SO_4)$ (compound **2**).

Compound **2** crystallizes in the non-centrosymmetric space group *P2₁*. The structure determination was performed using Superflip and the charge flipping algorithm using the *P1* space group. The determined electron density was then analysed to evidence symmetry operators as described by Palatinus *et al.*[49] This method led to the *P2₁* space group. All the attempts of structural determination in a centro symmetric space group (using charge flipping but also direct methods) were unsuccessful, supporting the assumption of an acentric space group and this despite the lack of high angle diffraction. This is further confirmed by SHG measurements (see below).The crystal structure of compound **2** can be described by 2 Cu, 1 S, 7 O, 12 C independent atoms. All the atomic positions were refined and then atomic displacement parameters (ADP) were considered as anisotropic for copper and sulfur atoms and isotropic for all remaining atoms. In addition, 25 independent hydrogen atoms were further introduced using geometric considerations to fill the carbon environment. As for oxygen atoms, bond valence sum calculations indicated low values for O2, O3 and O7 attributed to the presence of H atoms. Each of these O are surrounded by 3 copper atoms and the hydrogen is building a OCu_3H tetrahedron. The position of the H atoms was determined based on these geometrical considerations and restricted in link to their O first

neighbour. The model results in the elemental formula $Cu_2(OH)_3(C_{12}H_{25}SO_4)$. Since the space group is non-centrosymmetric, a twin law corresponding to an inversion center has been introduced and the ratio of the possible twin domains (*i.e.* the Flack parameters) was refined to 0.26(9)/0.74(9). Final reliability factors and details of the refinement are reported in Table 1 and the atomic parameters of the crystal **2** are summarized in Tables S2a and S2b.

Compound **2** consists in layers of copper hydroxide of botallackite type structure, separated by dodecylsulfate ions, with an interlamellar distance of 26.93 Å (Figure 3). The dodecylsulfate molecules are coordinated to the layers by the sulfate group in κ^1-μ_3 position. The structure resembles one recently reported with aromatic sulfonate molecules, yet to the best of our knowledge, it is the first time the crystal structure of a sulfate-containing layered copper hydroxide is reported, despite the fact that $Cu_2(OH)_3(C_{12}H_{25}SO_4)$ is often used as a precursor for intercalation compounds.[5,25,26]

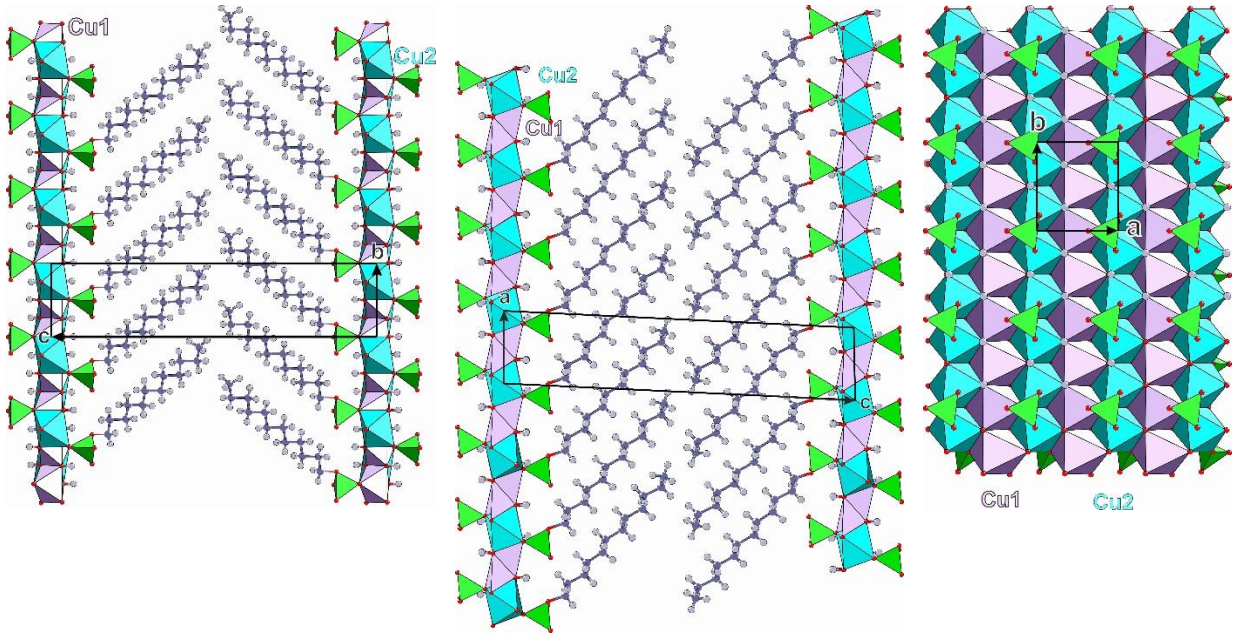

Figure 3. Views of the structure of **2** $Cu_2(OH)_3(C_{12}H_{25}SO_4)$ left: along *a*; middle: along *b*. Structure of the inorganic layer, (*ab*) plane (right). Cu (purple (Cu1) and blue (Cu2)), O (red), S (green), C (grey), H (white).

One peculiar aspect of the structure of **2** is that it crystallizes in a non-centrosymmetric space group. The non-centrosymmetry comes from the fishbone arrangement of the alkyl chains in the interlamellar spacing. This arrangement is different from the one which was classically and empirically drawn, where the alkyl chains were simply interdigitated in the interlamellar spacing.[41,50,51] This compound constitutes one relatively rare example of a chiral compound obtained from achiral building blocks,[52–54] even though, as in most of the cases reported in the literature,[54] the bulk sample of **2** likely contains both enantiomorphs (*i.e.* of opposite handedness). Interestingly, $Cu_2(OH)_3(OAc)\cdot H_2O$ also crystallizes in a non-centrosymmetric space group ($P2_1$),[42] with the acetate molecules forming a fish-bone arrangement, contrarily to what was initially inferred by calculations ($P2_1/m$).[55] Here, even though it could not be obtained *via* a crystal to crystal transformation from $Cu_2(OH)_3(OAc)\cdot H_2O$, $Cu_2(OH)_3(C_{12}H_{25}SO_4)$ crystallizes in the same non-centrosymmetric crystal space group as $Cu_2(OH)_3(OAc)\cdot H_2O$. It is worth noting here that layered copper hydroxides functionalized by sulfonate molecules, as reported by Fujita *et al.*, crystallize in centrosymmetric space groups, even though the synthetic procedure is similar to the one described here.[32] Hence, functionalizing the hydroxide layers with sulfate instead of sulfonate has a significant influence on the structure that can lead to different properties.

Non-Linear Optics

In order to fully ascertain the non-centrosymmetry of the structure of **2**, Non-Linear Optical microscopy was performed. Measurements on a single crystal show a clear Second Harmonic Generation signal (Figure S6). To avoid any false-positive signal due to surface Second Harmonic Generation (all the more since the thickness of the crystals is small), we managed to record SHG intensity as a function of thickness on a partially cleaved crystal (Figure 4). The enhancement of the SHG signal with the thickness rules out a surface effect. Since non-centrosymmetry is a necessary condition for Non-Linear Optical activity, the observation of a clear SHG signal for **2** confirms its non-centrosymmetry.

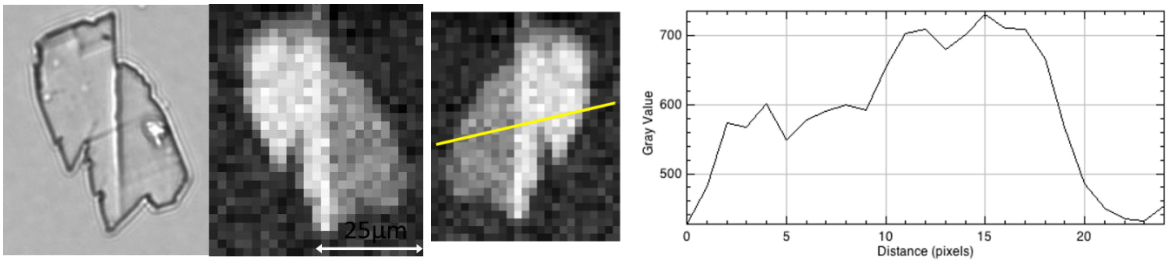

Figure 4. Non-Linear Optical microscopy observation of a partially cleaved crystal of **2**. From left to right : optical microscopy image, SHG intensity image, and SHG intensity profile (for observation reasons, the image and profile are flipped with respect to optical microscopy image).

Comparison with classical method and morphology control

The method used to synthesize the compound **2** enables to obtain more than 800 mg for each synthesis, with a yield of about 40%. This synthesis does not involve any pH adjustment like the one used by Okazaki *et al.*[50] Compared to the « classical » ion-exchange method from $Cu_2(OH)_3(OAc)\cdot H_2O$,[41] this one-step hydrolysis method enables to increase greatly the crystallite size (Figure 5).

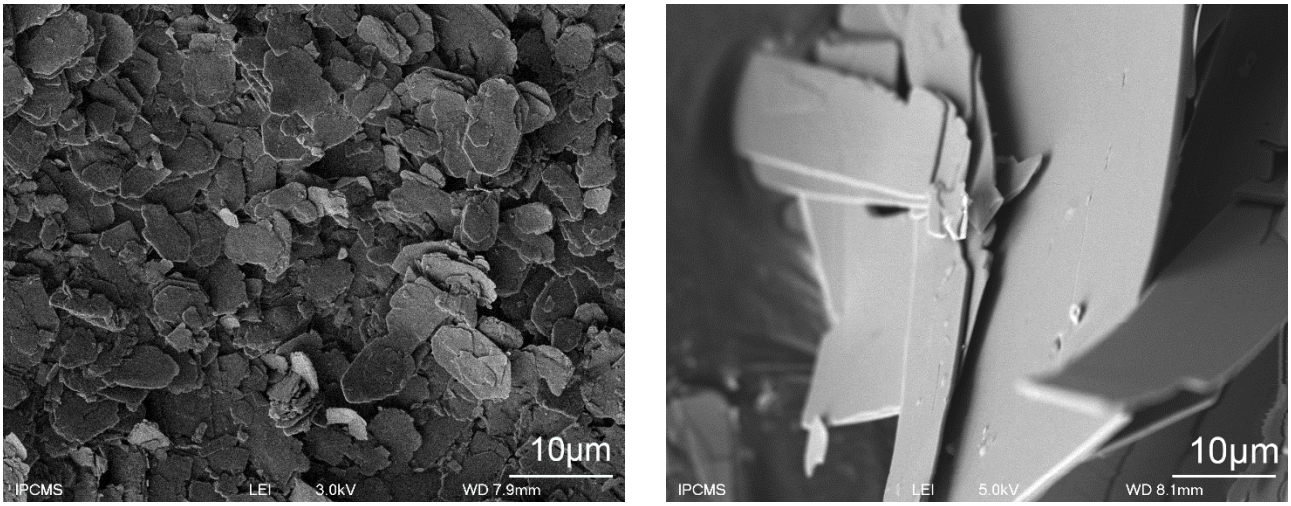

Figure 5. SEM image of $Cu_2(OH)_3(C_{12}H_{25}SO_4)$ obtained *via* ion exchange from $Cu_2(OH)_3(OAc)\cdot H_2O$ (left) and *via* the one-step hydrolytic synthesis described in the present work (right).

Finally, it is worth noticing that depending on the water/ethanol ratio and of the reaction temperature, it was possible to control the morphology of the $Cu_2(OH)_3(DS)$ crystallites. Using up to 30% of ethanol, as described in the experimental part, the crystallites have the classical regular platelet shape. For an ethanol content larger than 40%, associated with a lower reaction temperature (30°C instead of 60°C), the crystallites adopt a "butterfly" morphology (Figure 6). We checked by Rietveld refinements of the powder X-ray diffraction data that the crystal structure does not change (Figure S1).

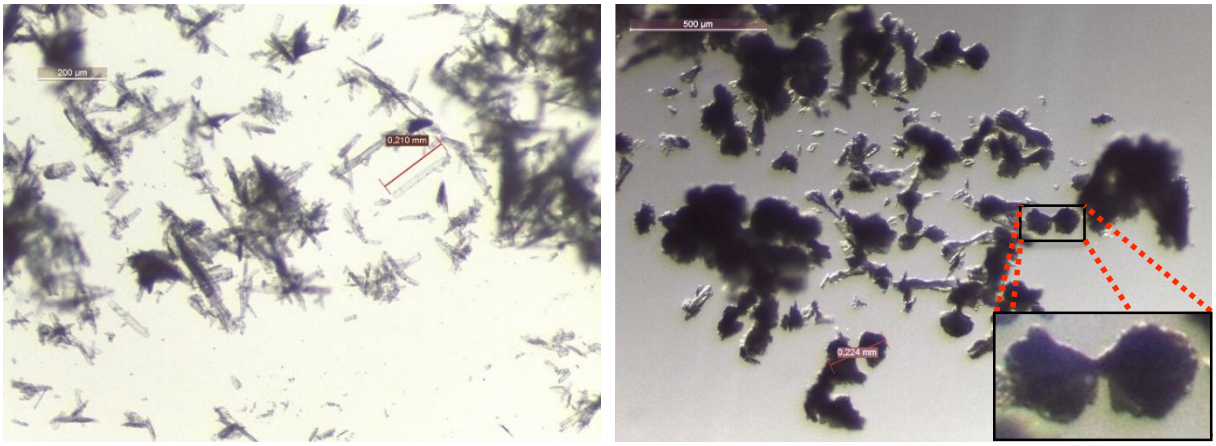

Figure 6. Optical images of the regular platelet morphology (left) and of the butterfly morphology (right).

Magnetic properties

The magnetic properties of compounds **1** and **2** were recorded in the range 1.8-300 K under a dc magnetic field of 5000 G.

The magnetic properties of compound **1** are presented in Figure 7. The fit of the $1/\chi = f(T)$ curve in the high-temperature region (above 200 K) leads to a Curie constant of 1.73 emu·K·mol^{-1} (*i.e.* 0.58 emu·K·mol^{-1} *per* Cu(II) ion, within the range of expected values[56]) and negative Weiss temperature of -77 K, which indicates dominant antiferromagnetic interactions. The $\chi = f(T)$ for compound **1** indicates a paramagnetic behaviour on the whole temperature range with short-range interactions. The curve presents a sharp maximum at 10.5 K with a very broad shoulder centered around 70 K. This peculiar shape, with two, more or less defined, peaks in $\chi = f(T)$ has already been observed in other diamond-like Cu(II) hydroxide chains, with sulfonate and acetate ligands,[47] or for the related $Cu_3(OH)_2(CO_3)_2$ azurite.[48]

The $\chi = f(T)$ curve for **1** could be fitted above 7 K, considering isolated chains (separated by the long dodecylsulfate molecules), and the spin topology schematized on figure 8. Below 7 K, the

model used is too simplified to be valid, because other intrachain or 3D interchain interactions are likely to be taken into account in this temperature range and because of the finite size of the model.

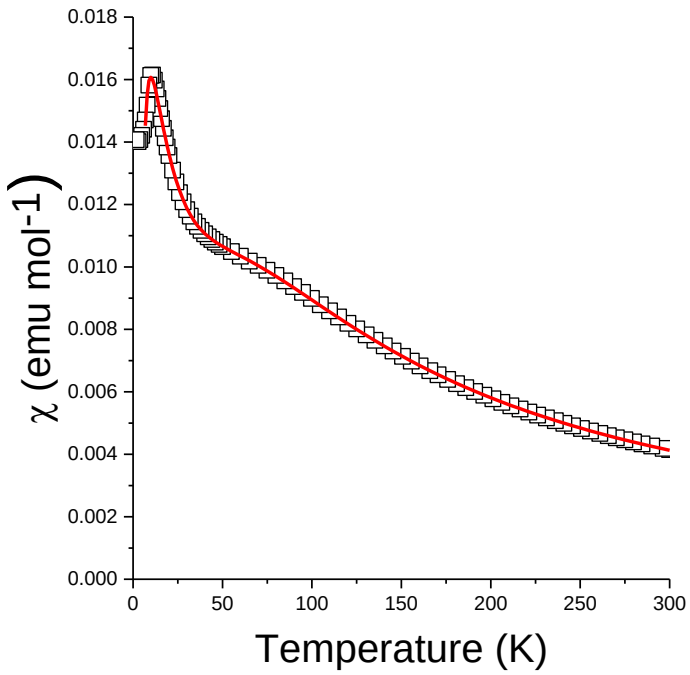

Figure 7. χ = f(T) curve at 5000 G for compound **1** (open squares: experimental points, full red line: best fit).

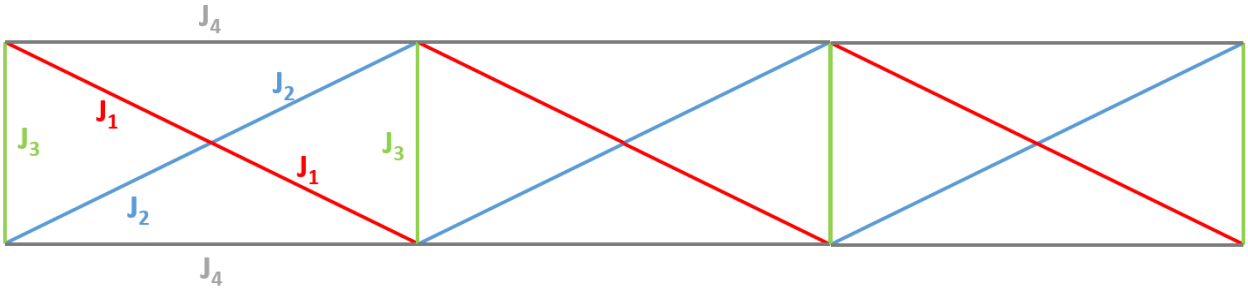

Figure 8. Spin topology considered for **1** above 13 K. This topology is identical to the one used by Fujita *et al.* for related diamond-like chain compounds bearing sulfonate molecules.[47]

The fit was performed considering the following Hamiltonian for spin-spin interactions :

$\hat{\mathbf{H}} = \Sigma - J_{ij}\, \hat{\mathbf{S}}_\mathbf{i}\, \hat{\mathbf{S}}_\mathbf{j}$. We considered a ring of twelve spins to reproduce the chain behaviour without edge effect. The numerical resolution of the Hamiltonian was carried out by using the program SPIN including a refinement routine.[57] A very good adjustment of the experimental data was obtained with the refined values : J_1 = 11(6) cm^{-1}, J_2 = -75(1) cm^{-1}, J_3 = -52(2) cm^{-1}, J_4 = 28(2) cm^{-1} and g = 2.29(3) (the fit was performed with a single g factor for the two different copper ions to limit over-parameterization). Standard deviations on J_i values are quite high due to important correlations between parameters. Given the fact that several exchange pathways exist between two spin carriers, it is here difficult and beyond the scope of this study to perform a clear correlation between the *J* values determined and the structure of the compound. Yet it is worth noticing that the *J* values are moderate, and within the usually observed range for Cu-O-Cu (OH, (κ^1-μ_2)-sulfate or (κ^1-μ_2)-carboxylate bridges) or Cu-OCO-Cu (((κ^1-κ^1)-μ_2)-carboxylate) motives.[47,58,59] In particular, it is noteworthy that the Cu-Cu interaction *via* the ((κ^1-κ^1)-μ_2)-carboxylate (J_4) is ferromagnetic, as expected for a *syn-anti* carboxylate.[60] Clearly, the peculiar behavior of compound **1** can be explained by the competition between ferromagnetic and antiferromagnetic nearest neighbour exchange interactions.

As for compound **2**, the fit of the $1/\chi$ = f(T) curve in the high-temperature region (above 200 K) leads to a Curie constant of 0.89 emu·K·mol^{-1} (*i.e.* 0.45 emu·K·mol^{-1} *per* Cu(II) ion, within the range of expected values[56]) and very small negative Weiss temperature of -0.3 K, which indicates dominant antiferromagnetic interactions. Approximating the triangular magnetic lattice as being regular, the χ = f(T) can be fitted using the high-temperature series expansion for a S = ½ Heisenberg 2D triangular lattice (Figure 9) for T > 20 K.[61,62]

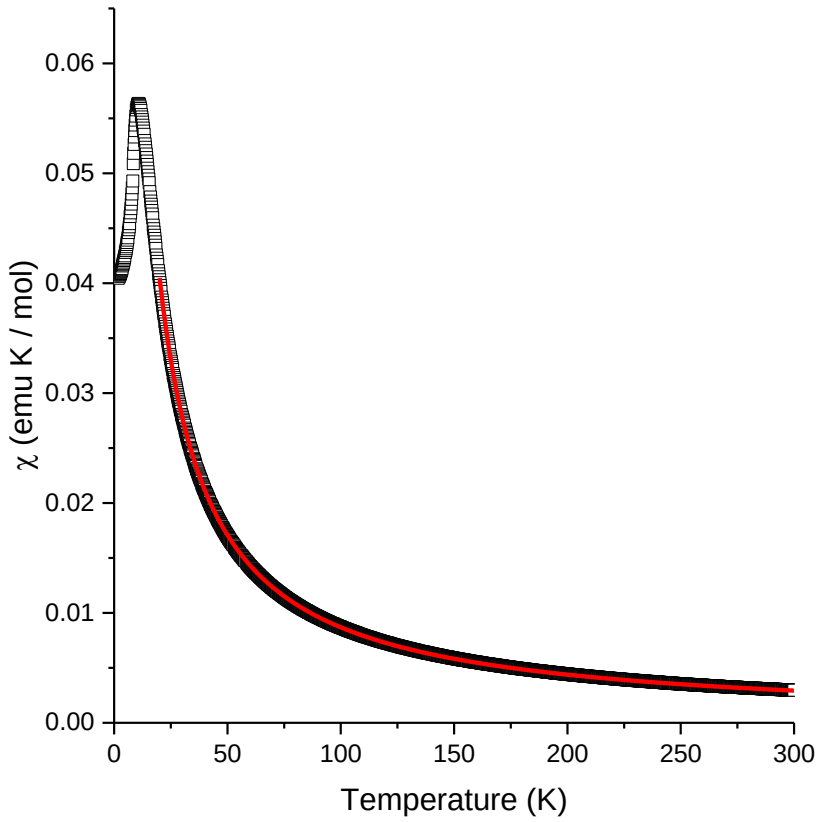

Figure 9. χ = f(T) curve at 5000 G for compound **2** (open squares: experimental points, full red line: best fit).

The best fit provides J = -0.40(1) cm^{-1} and g = 2.17(1). The exchange interaction is significantly smaller (by two orders of magnitude) than the ones obtained by Fujita for a series of layered hydroxides containing aromatic sulfonates.[32] The sharp maximum observed around 11 K in the χ = f(T) curve and the very abrupt decrease of χT = f(T) (Figure S7), can be associated with the occurrence of a long-range (3D) antiferromagnetic ordering. The ordering temperature can be determined precisely from the maximum of the in-phase susceptibility (Figure S8) leading to T_N

= 10.8 K. This value is slightly higher than the one determined recently for an analogous compound (synthesized by confined condensation, a totally different approach, and for which no crystal structure could be obtained) (T_N = 8 K).[33] The magnetization *vs.* field curve at 1.8 K shows a clear spin-flop transition for a critical field of 2 T (Figure 10) which supports an antiferromagnetic ordering at low temperature in compound **2**.

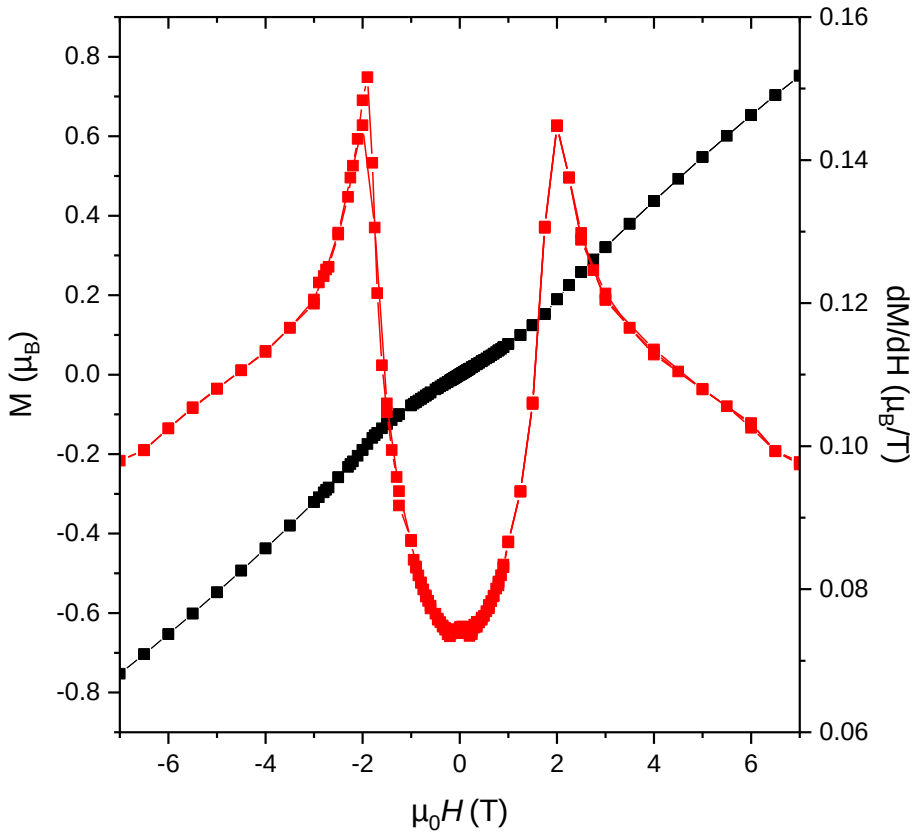

Figure 10. M = f(H) (black squares) and dM/dH = f(H) (red squares) at 1.8 K for **2**. Full lines are just guides for the eye.

Conclusion.

Single crystals of 1D and 2D copper hydroxides bearing dodecylsulfate molecules have been obtained by a hydrolysis method from copper acetate. This method has already been employed to obtain single crystals of $Cu_2(OH)_3(OAc)\cdot H_2O$,[42] various layered copper hydroxides containing aromatic sulfonates[32] and copper hydroxide distorted diamond chains bearing sulfonate molecules[47] but to the best of our knowledge, it is the first time this method is proved efficient to obtain single crystal of sulfate containing low dimensional copper hydroxide based hybrids.

The structure determination of $Cu_2(OH)_3(C_{12}H_{25}SO_4)$ is particularly noteworthy since this compound is widely used for further functionalization by ion-exchange reaction. Interestingly, X-ray structure analysis and NLO measurement clearly indicate that it crystallizes in a non-centrosymmetric space group just like the parent compound $Cu_2(OH)_3(OAc)\cdot H_2O$, contrarily to what was observed for layered copper hydroxides containing aromatic sulfonates.[32]

In addition, we isolated and fully characterized a 1D, ribbon-like, copper-hydroxide based compound, which can be considered as an intermediate between the "0D" copper acetate and the 2D $Cu_2(OH)_3(C_{12}H_{25}SO_4)$.

Extension of this hydrolysis approach to the preparation of highly crystalline hydroxide-based low dimensional hybrids networks with other transition metal ions is currently under study.

Supporting Information. Powder X-Ray diffraction diagram of **2** with butterfly morphology. Powder X-Ray diffraction diagram of the blueish precipitate and compound **1**. Powder X-Ray diffraction diagram and SEM images resulting from attempts of single-crystal to single-crystal functionalization of $Cu_2(OH)_3(OAc)\cdot H_2O$. IR spectra of the blueish precipitate and compound **1**.

Positional parameters and Atomic Displacement Parameters for **1** and **2**. Second Harmonic Generation signal for **2**. $\chi T = f(T)$ and ac susceptibility data for compound **2**.

CCDC 1588057 and 1588059 contains the supplementary crystallographic data for this paper.

Corresponding Author.

*E-mail : rogez@unistra.fr

Author Contributions.

The manuscript was written through contributions of all authors. All authors have given approval to the final version of the manuscript.

Ackowledgements.

The authors thank the CNRS, the Université de Strasbourg, the ENSICAEN and the Agence Nationale de la Recherche (contract N° ANR-14-CE07-0004-01 (HYMN)) and the Labex NIE (ANR-11-LABX-0058_NIE within the Investissement d'Avenir program ANR-10-IDEX-0002-02) for financial support. We thank Dr. T. Buffeteau (CNRS-University of Bordeaux, France) for interesting discussions.

References.

(1) Fernandes, F. M.; Baradari, H.; Sanchez, C. Integrative Strategies to Hybrid Lamellar Compounds: An Integration Challenge. *Appl. Clay Sci.* **2014**, *100*, 2–21.
(2) *Functional Hybrid Materials*; Gómez-Romero, P., Sanchez, C., Eds.; Wiley-VCH: Weinheim, 2004.
(3) Clemente-León, M.; Coronado, E.; Martí-Gastaldo, C.; Romero, F. M. Multifunctionality in Hybrid Magnetic Materials Based on Bimetallic Oxalate Complexes. *Chem. Soc. Rev.* **2011**, *40* (2), 473–497.
(4) Leroux, F.; Besse, J.-P. In *Clay Surfaces: Fundamentals and Applications*; Wypych, F., Satyanarayana, K. G., Eds.; Elsevier: London, 2004; pp 459–495.

(5) Rogez, G.; Massobrio, C.; Rabu, P.; Drillon, M. Layered Hydroxide Hybrid Nanostructures: A Route to Multifunctionality. *Chem. Soc. Rev.* **2011**, *40* (2), 1031–1058.
(6) Ley, C.; Brendlé, J.; Miranda, M.; Allonas, X. Spectroscopic Studies of the Interactions between a Cationic Cyanine Dye and a Synthetic Phyllosilicate: From Photophysics to Hybrid Materials. *Langmuir* **2017**, *33* (27), 6812–6818.
(7) Liu, J.; Zhang, G. Recent Advances in Synthesis and Applications of Clay-Based Photocatalysts: A Review. *Phys. Chem. Chem. Phys.* **2014**, *16* (18), 8178–8192.
(8) Lacroix, P. G.; Clément, R.; Nakatani, K.; Zyss, J.; Ledoux, I. Stilbazolium-MPS_3 Nanocomposites with Large Second-Order Optical Nonlinearity and Permanent Magnetization. *Science* **1994**, *263* (5147), 658–660.
(9) Clément, R.; Léaustic, A. In *Magnetism: Molecules to Materials II. Molecule-based Materials*; Miller, J. S., Drillon, M., Eds.; Wiley-VCH: Weinheim, 2001.
(10) Schaak, R. E.; Mallouk, T. E. Perovskites by Design: A Toolbox of Solid-State Reactions. *Chem. Mater.* **2002**, *14* (4), 1455–1471.
(11) Mitzi, D. B. Hybrid Organic-Inorganic Electronics. In *Functional Hybrid Materials*; Romero, P.-G., Sanchez, C., Eds.; Wiley-VCH, 2004; pp 347–390.
(12) Intissar, M.; Segni, R.; Payen, C.; Besse, J.-P.; Leroux, F. Trivalent Cation Substitution Effect into Layered Double Hydroxides $Co_2Fe_y\ Al_{1-y}(OH)_6Cl{\cdot}nH_2O$: Study of the Local Order: Ionic Conductivity and Magnetic Properties. *J. Solid State Chem.* **2002**, *167* (2), 508–516.
(13) Coronado, E.; Galán-Mascarós, J. R.; Martí-Gastaldo, C.; Ribera, A.; Palacios, E.; Castro, M.; Burriel, R. Spontaneous Magnetization in Ni−Al and Ni−Fe Layered Double Hydroxides. *Inorg. Chem.* **2008**, *47* (19), 9103–9110.
(14) Bristowe, N. C.; Varignon, J.; Fontaine, D.; Bousquet, E.; Ghosez, P. Ferromagnetism Induced by Entangled Charge and Orbital Orderings in Ferroelectric Titanate Perovskites. *Nat. Commun* **2015**, *6*, 6677.
(15) Pardo, E.; Train, C.; Liu, H.; Chamoreau, L.-M.; Dkhil, B.; Boubekeur, K.; Lloret, F.; Nakatani, K.; Tokoro, H.; Ohkoshi, S.; et al. Multiferroics by Rational Design: Implementing Ferroelectricity in Molecule-Based Magnets. *Angew. Chem. Int. Ed.* **2012**, *51* (33), 8356–8360.
(16) Polyakov, A. O.; Arkenbout, A. H.; Baas, J.; Blake, G. R.; Meetsma, A.; Caretta, A.; van Loosdrecht, P. H. M.; Palstra, T. T. M. Coexisting Ferromagnetic and Ferroelectric Order in a $CuCl_4$-Based Organic–Inorganic Hybrid. *Chem. Mater.* **2012**, *24* (1), 133–139.
(17) Kundys, B.; Lappas, A.; Viret, M.; Kapustianyk, V.; Rudyk, V.; Semak, S.; Simon, C.; Bakaimi, I. Multiferroicity and Hydrogen-Bond Ordering in $(C_2H_5NH_3)_2CuCl_4$ Featuring Dominant Ferromagnetic Interactions. *Phys. Rev. B* **2010**, *81* (22), 224434.
(18) Evrard, Q.; Chaker, Z.; Roger, M.; Sevrain, C. M.; Delahaye, E.; Gallart, M.; Gilliot, P.; Leuvrey, C.; Rueff, J.-M.; Rabu, P.; et al. Layered Simple Hydroxides Functionalized by Fluorene-Phosphonic Acids: Synthesis, Interface Theoretical Insights, and Magnetoelectric Effect. *Adv. Funct. Mater.* **2017**, 1703576.
(19) Ogawa, M.; Kuroda, K. Photofunctions of Intercalation Compounds. *Chem. Rev.* **1995**, *95* (2), 399–438.
(20) Abid, H.; Samet, A.; Dammak, T.; Mlayah, A.; Hlil, E. K.; Abid, Y. Electronic Structure Calculations and Optical Properties of a New Organic–inorganic Luminescent Perovskite: $(C_9H_{19}NH_3)_2PbI_2Br_2$. *J. Lumin.* **2011**, *131* (8), 1753–1757.

(21) Sánchez-Ochoa, F.; Cocoletzi, G. H.; Canto, G. Trapping and Diffusion of Organic Dyes inside of Palygorskite Clay: The Ancient Maya Blue Pigment. *Microporous Mesoporous Mater.* **2017**, *249*, 111–117.
(22) Aristilde, L.; Lanson, B.; Miéhé-Brendlé, J.; Marichal, C.; Charlet, L. Enhanced Interlayer Trapping of a Tetracycline Antibiotic within Montmorillonite Layers in the Presence of Ca and Mg. *J. Colloid Interface Sci.* **2016**, *464*, 153–159.
(23) Stimpfling, T.; Vialat, P.; Hintze-Bruening, H.; Keil, P.; Shkirskiy, V.; Volovitch, P.; Ogle, K.; Leroux, F. Amino Acid Interleaved Layered Double Hydroxides as Promising Hybrid Materials for AA2024 Corrosion Inhibition. *Eur. J. Inorg. Chem.* **2016**, *2016* (13–14), 2006–2016.
(24) García-González, N.; Frontana-Uribe, B. A.; Ordoñez-Regil, E.; Cárdenas, J.; Morales-Serna, J. A. Evaluation of Fe^{3+} Fixation into Montmorillonite Clay and Its Application in the Polymerization of Ethylenedioxythiophene. *RSC Adv.* **2016**, *6* (98), 95879–95887.
(25) Delahaye, É.; Eyele-Mezui, S.; Bardeau, J.-F.; Leuvrey, C.; Mager, L.; Rabu, P.; Rogez, G. New Layered Organic-Inorganic Magnets Incorporating Azo Dyes. *J. Mater. Chem.* **2009**, *19* (34), 6106–6115.
(26) Bourzami, R.; Eyele-Mezui, S.; Delahaye, E.; Drillon, M.; Rabu, P.; Parizel, N.; Choua, S.; Turek, P.; Rogez, G. New Metal Phthalocyanines/Metal Simple Hydroxide Multilayers: Experimental Evidence of Dipolar Field-Driven Magnetic Behavior. *Inorg. Chem.* **2014**, *53* (2), 1184–1194.
(27) Fujita, W.; Awaga, K. Reversible Structural Transformation and Drastic Magnetic Change in a Copper Hydroxide Intercalation Compound. *J. Am. Chem. Soc.* **1997**, *119* (19), 4563–4564.
(28) Fujita, W.; Awaga, K. Magnetic Properties of $Cu_2(OH)_3$(Alkanecarboxylate) Compounds: Drastic Modification with Extension of the Alkyl Chain. *Inorg. Chem.* **1996**, *35* (7), 1915–1917.
(29) Demessence, A.; Yassar, A.; Rogez, G.; Miozzo, L.; Brion, S. D.; Rabu, P. Synthesis, Optical and Magnetic Properties of Hybrid α,α′-Oligothiophenecarboxylates/Transition Metal Hydroxide Multilayered Compounds. *J. Mater. Chem.* **2010**, *20* (42), 9401–9414.
(30) Kurmoo, M.; Kumagai, H.; Hughes, S. M.; Kepert, C. J. Reversible Guest Exchange and Ferrimagnetism (TC = 60.5 K) in a Porous Cobalt(II)−Hydroxide Layer Structure Pillared with Trans-1,4-Cyclohexanedicarboxylate. *Inorg. Chem.* **2003**, *42* (21), 6709–6722.
(31) Palamarciuc, O.; Delahaye, E.; Rabu, P.; Rogez, G. Microwave-Assisted Post-Synthesis Modification of Layered Simple Hydroxides. *New J. Chem.* **2014**, *38* (5), 2016–2023.
(32) Fujita, W. Convenient Crystal Growth, Structural Determination and Magnetic Studies of Layered Copper Hydroxides Containing Aromatic Sulfonates. *CrystEngComm* **2015**, *17* (47), 9193–9202.
(33) Park, S.-H.; Jung, M.-H.; Lee, Y.-J.; Huh, Y.-D. Confined Condensation Synthesis and Magnetic Properties of Layered Copper Hydroxide Frameworks. *Dalton Trans.* **2017**, *46* (10), 3363–3368.
(34) Delahaye, É.; Eyele-Mezui, S.; Diop, M.; Leuvrey, C.; Rabu, P.; Rogez, G. Rational Synthesis of Chiral Layered Magnets by Functionalization of Metal Simple Hydroxides with Chiral and Non-Chiral Ni(II) Schiff Base Complexes. *Dalton Trans.* **2010**, *39* (44), 10577–10580.
(35) Eyele-Mezui, S.; Delahaye, E.; Rogez, G.; Rabu, P. Functional Hybrid Materials Based on Layered Simple Hydroxide Hosts and Dicarboxylate Schiff Base Metal Complex Guests. *Eur. J. Inorg. Chem.* **2012**, No. 32, 5225–5238.

(36) Yamanaka, S.; Sako, T.; Seki, K.; Hattori, M. Anion Exchange Reactions in Layered Basic Copper Salts. *Solid State Ion.* **1992**, *53–56* (Part 1), 527–533.
(37) Yamanaka, S.; Sako, T.; Hattori, M. Anion-Exchange in Basic Copper Acetate. *Chem. Lett.* **1989**, *18* (10), 1869–1872.
(38) Rabu, P.; Rouba, S.; Laget, V.; Hornick, C.; Drillon, M. Ferro/Antiferromagnetism Mediated by Interlayer Organic Spacers in Layered Copper(II) Compounds. *Chem. Commun.* **1996**, *0* (10), 1107–1108.
(39) Laget, V.; Drillon, M.; Hornick, C.; Rabu, P.; Romero, F.; Turek, P.; Ziessel, R. Copper Hydroxide Based Organic/Inorganic Ferromagnets. *J. Alloys Compd.* **1997**, *262–263* (Supplement C), 423–427.
(40) Fujita, W.; Awaga, K.; Yokoyama, T. Controllable Magnetic Properties of Layered Copper Hydroxides, $Cu_2(OH)_3X$ (X=carboxylates). *Appl. Clay Sci.* **1999**, *15* (1), 281–303.
(41) Laget, V.; Hornick, C.; Rabu, P.; Drillon, M. Hybrid Organic-Inorganic Layered Compounds Prepared by Anion Exchange Reaction: Correlation between Structure and Magnetic Properties. *J. Mater. Chem.* **1999**, *9* (1), 169–174.
(42) Švarcová, S.; Klementová, M.; Bezdička, P.; Łasocha, W.; Dušek, M.; Hradil, D. Synthesis and Characterization of Single Crystals of the Layered Copper Hydroxide Acetate $Cu_2(OH)_3(CH_3COO)\cdot H_2O$. *Cryst. Res. Technol.* **2011**, *46* (10), 1051–1057.
(43) Petříček, V.; Dušek, M.; Palatinus, L. Crystallographic Computing System JANA2006: General Features. *Z. Für Krist. - Cryst. Mater.* **2014**, *229* (5), 345–352.
(44) Sheldrick, G. M. *SADABS, Bruker–Siemens Area Detector Absorption and Other Correction, Version 2008/1*; 2008.
(45) Sheldrick, G. M. *SADABS. Program for Empirical Absorption Correction*; University of Göttingen, Germany, 1996.
(46) Palatinus, L.; Chapuis, G. SUPERFLIP – a Computer Program for the Solution of Crystal Structures by Charge Flipping in Arbitrary Dimensions. *J. Appl. Crystallogr.* **2007**, *40* (4), 786–790.
(47) Fujita, W.; Tokumitu, A.; Fujii, Y.; Kikuchi, H. Crystal Growth, Structures and Magnetic Properties of Copper Hydroxide Compounds with Distorted Diamond Chain Magnetic Networks. *CrystEngComm* **2016**, *18* (44), 8614–8621.
(48) Kikuchi, H.; Fujii, Y.; Chiba, M.; Mitsudo, S.; Idehara, T.; Tonegawa, T.; Okamoto, K.; Sakai, T.; Kuwai, T.; Ohta, H. Experimental Observation of the 1/3 Magnetization Plateau in the Diamond-Chain Compound $Cu_3(CO_3)_2(OH)_2$. *Phys. Rev. Lett.* **2005**, *94*, 227201.
(49) Palatinus, L.; van der Lee, A. Symmetry Determination Following Structure Solution in *P1*. *J. Appl. Crystallogr.* **2008**, *41* (6), 975–984.
(50) Okazaki, M.; Toriyama, K.; Tomura, S.; Kodama, T.; Watanabe, E. A Monolayer Complex of Cu2(OH)3C12H25SO4 Directly Precipitated from an Aqueous SDS Solution. *Inorg. Chem.* **2000**, *39* (13), 2855–2860.
(51) Park, S.-H.; Lee, C. E. Layered Copper Hydroxide N-Alkylsulfonate Salts: Synthesis, Characterization, and Magnetic Behaviors in Relation to the Basal Spacing. *J. Phys. Chem. B* **2005**, *109* (3), 1118–1124.
(52) Janiak, C. Engineering Coordination Polymers towards Applications. *Dalton Trans.* **2003**, *0* (14), 2781–2804.
(53) Gil-Hernández, B.; Höppe, H. A.; Vieth, J. K.; Sanchiz, J.; Janiak, C. Spontaneous Resolution upon Crystallization of Chiral La(III) and Gd(III) MOFs from Achiral Dihydroxymalonate. *Chem. Commun.* **2009**, *46* (43), 8270–8272.

(54) Ma, L.; Abney, C.; Lin, W. Enantioselective Catalysis with Homochiral Metal–organic Frameworks. *Chem. Soc. Rev.* **2009**, *38* (5), 1248–1256.
(55) Masciocchi, N.; Corradi, E.; Sironi, A.; Moretti, G.; Minelli, G.; Porta, P. Preparation, Characterization, Andab InitioX-Ray Powder Diffraction Study of $Cu_2(OH)_3(CH_3COO)\cdot H_2O$. *J. Solid State Chem.* **1997**, *131* (2), 252–262.
(56) Carlin, R. L. *Magnetochemistry*; Springer-Verlag: Berlin, 1986.
(57) Legoll, P.; Drillon, M.; Rabu, P.; Maingot, F. *SPIN 2.3*; Université Louis Pasteur, Strasbourg, 1996.
(58) Gómez-García, C. J.; Escrivà, E.; Benmansour, S.; Borràs-Almenar, J. J.; Folgado, J.-V.; Ramírez de Arellano, C. Alternating Ferro/Antiferromagnetic Copper(II) Chain Containing an Unprecedented Triple Formato/Hydroxido/Sulfato Bridge. *Inorg. Chem.* **2016**, *55* (5), 2664–2671.
(59) Crawford, V. H.; Richardson, H. W.; Wasson, J. R.; Hodgson, D. J.; Hatfield, W. E. Relation between the Singlet-Triplet Splitting and the Copper-Oxygen-Copper Bridge Angle in Hydroxo-Bridged Copper Dimers. *Inorg. Chem.* **1976**, *15* (9), 2107–2110.
(60) Murugesu, M.; Clérac, R.; Pilawa, B.; Mandel, A.; Anson, C. E.; Powell, A. K. Ferromagnetic Interactions Mediated by Syn–anti Carboxylate Bridging in Tetranuclear Copper(II) Compounds. *Inorganica Chim. Acta* **2002**, *337*, 328–336.
(61) Rushbrooke, G. S.; Wood, P. J. On the High-Temperature Susceptibility for the Heisenberg Model of a Ferromagnet. *Proc. Phys. Soc. Sect. A 68*, 1161–1169.
(62) Navarro, R. In *Magnetic Properties of Layered Transition Metal Compounds*; de Jongh, L. J., Ed.; Kluwer Academic Publishers: Dordrecht, 1990.

For Table of Contents Use Only

A non-centrosymmetric Cu(II) layered hydroxide: synthesis, crystal structure, non-linear optical and magnetic properties of $Cu_2(OH)_3(C_{12}H_{25}SO_4)$

Quentin Evrard, Cédric Leuvrey, Pierre Farger, Emilie Delahaye, Pierre Rabu, Grégory Taupier, Kokou Dodzi Dorkenoo, Jean-Michel Rueff, Nicolas Barrier, Olivier Pérez, Guillaume Rogez *

Single-crystals of the layered copper hydroxide dodecylsulfate $Cu_2(OH)_3(C_{12}H_{25}SO_4)$ have been obtained by controlled hydrolysis of an aqueous copper acetate solution. This compound crystallizes in the non-centrosymmetric space group $P2_1$. An intermediate compound with a ribbon-like structure, of formula $Cu_3(C_{12}H_{25}SO_4)_2(CH_3COO)_2(OH)_2(H_2O)_2$, was isolated and fully characterized. The magnetic properties of both compounds are thoroughly analyzed.